

RESEARCH ARTICLE

Evaluation of Centralized and Distributed Energy Storage Systems in Residential Microgrid Topologies

Sezai Polat¹, Emrah Bıyık²

¹Directorate of Construction Works and Technical, İzmir Katip Çelebi University, İzmir, Türkiye

²Department of Energy Systems Engineering, Yaşar University Faculty of Engineering, İzmir, Türkiye

Cite this article as: S. Polat and E. Bıyık, "Evaluation of centralized and distributed energy storage systems in residential microgrid topologies," *Turk J Electr Power Energy Syst.*, 2025; 5(1), 30-40.

ABSTRACT

The determination of both the connection topology and capacity sizing of the battery energy storage system (BESS) in a microgrid is crucial when considering energy bills and reliability indicators, as the usage type of the BESS affects investment and energy costs. In this study, the performances of individual and shared BESSs are compared across different price tariffs in a multi-microgrid structure designed using historical real data and existing prosumer solar homes. To illustrate the effects of the integrated BESS and grid outages on the cost of energy and net present cost (NPC), a BESS is first integrated into the selected solar home as a sample. The calculations are then made assuming an outage in the grid connected to the selected home with the integrated BESS. In the proposed system topology, which utilizes five selected solar homes with a shared BESS, the NPCs were found to be 51%, 28%, and 37% lower compared to individual systems for real-time pricing (RTP), flat price tariff (FPT), and time-of-use pricing (ToU), respectively. Furthermore, in modeling these grid interruptions, which are a real-life condition, system reliability indices such as system average interruption duration index and system average interruption frequency index were considered in the system sizing and cost optimization. When these indices were taken into account, similar reductions were observed compared to the individual system: 9% in RTP, 26% in FPT, and 61% in ToU, respectively.

Index Terms—Battery energy storage, cost of energy, microgrid topology, net present cost

I. INTRODUCTION

The usage of renewable energies, which is beginning to replace the use of conventional sources, is becoming more common. However, the uncertainty of renewable energy sources (RESs) causes a decrease in the reliability of energy supply. For this reason, energy systems should be designed considering these uncertainties to ensure uninterrupted energy. Hybrid energy systems (HES), which have been extensively studied recently, have emerged as a good method to ensure energy continuity [1]. Hybrid RES-based microgrid systems provide a suitable arrangement to solve the reliability and cost relationship issue [2]. The design of HES is important to ensure the use of renewable energies and continuous energy supply. The continuity of energy has become increasingly significant for distribution companies as well. Consequently, the most well-known reliability indices, system average interruption duration index (SAIDI) and customer average interruption duration index (CAIDI), have commonly been defined by energy providers as interruption measurement methods in recent years [3]. Optimal hybrid renewable energy

systems (HRES), which are reliable and cost-effective, are designed through the accurate sizing of each component [4]. The design of a HES is more complex than a single-source energy system due to the stochastic load demand and renewable energy variables and parameters in optimal design [5]. An optimal sizing method could help to reduce complexity and achieve minimum capital costs through the use of all system equipment. Currently, several commercial software, such as hybrid optimization model for multiple energy resources (HOMER Pro), renewable energy and energy efficiency technology screen (RETScreen), PVSyst software, Hybrid2, iHOGA software, and transient system simulation tool (TRNSYS), are among the most common in the literature for designing, sizing, and optimizing renewable energies, focusing on technical and economic evaluation [6]. HOMER Pro among these design software stands out because it fulfills the requirements for three basic system design tasks: simulation, optimization, and design, as well as various analyses [7-11]. As mentioned in [12], the use of a battery energy storage system (BESS) can ensure resilience and optimize microgrids.

Corresponding author: Sezai Polat E-mail: sezai.polat@ikcu.edu.tr



Content of this journal is licensed under a Creative Commons Attribution (CC BY) 4.0 International License.

Received: October 08, 2024
Revision Requested: October 15, 2024
Last Revision Received: October 21, 2024
Accepted: October 24, 2024
Publication Date: December 2, 2024

BESS integration offers numerous benefits for stakeholders in the distribution system. These benefits can be categorized into two groups. The first group, which focuses on the electricity grid operator, improves the stability, sustainability, and reliability of RESs in power systems. The second group, which addresses the end user's perspective, reduces electricity costs and the number of interruptions by storing energy during periods of excess renewable generation and cheaper electricity for later usage when renewable generation is scarce and electricity prices are higher. Another key application that emerges in system design is the use of equipment sharing to reduce energy costs and investment expenses. It can be predicted that the benefits of integrating BESS into microgrids will also be advantageous in energy-sharing systems [13]. In this respect, the idea of energy sharing among microgrids has gained prominence, and with advancements in technology, the sharing of BESSs has been extensively investigated in recent studies [14, 15-18].

The emergence of the concept of energy exchange or energy sharing in microgrids has brought the focus to the optimal sizing of BESS for integration into HRES. As the prices of BESSs decrease, their usage has become more widespread. Beyond their conventional use during grid power outages, BESSs are now utilized for islanding, grid balancing, peak shaving, and behind-the-meter energy market participation. These use cases can be briefly summarized as follows:

Islanding: BESS is utilized in rural areas alongside RESs [19].

Grid balancing: Maintains grid balance, reducing distribution grid investment needs [20].

Peak shaving: Reduces grid usage during peak hours by charging BESS when energy is cheap and using it later [21].

Behind-the-meter market: BESS stores excess photovoltaic (PV) energy for use when renewable generation is unavailable, like in the evening [22].

Fig. 1 shows energy flow in a solar prosumer with BESS.

Main Points

- This study integrates HOMER software with real world reliability indices to model and optimize shared battery energy storage for solar home microgrids, using actual load and solar generation profiles.
- This study examines the benefits of shared battery energy storage systems in reducing energy use and improving grid reliability, as measured by SAIDI and SAIFI. The study also looks at energy costs, investment factors, and system performance under different electricity pricing.
- The research examines new configurations for multi-microgrids using a shared battery energy storage system topology. It contributes to the existing literature and suggests new ideas for microgrid applications.

The power electronics topologies for the BESS integrated with the PV system differ from those of traditional grid-connected BESSs due to the variety of PV system connection types. This study focuses on the use of low-power batteries, as those suitable for solar homes are considered.

Fig. 2 depicts the two most commonly used connection schemes for batteries in residential rooftop PV systems.

The battery pack is connected to the AC system via a DC/DC and DC/AC converter. Thanks to its high flexibility, the topology shown in Fig. 2a can be easily integrated with an existing PV system. The BESS is connected between a DC/DC converter, which includes the PV system's maximum power point tracker (MPPT), and the DC/AC inverter, as depicted in Fig. 2b. This connection type does not require a separate DC/AC converter for the battery system, making it more advantageous in terms of DC/AC efficiency. However, it has limitations when it comes to integrating with an existing system [25].

This study aims to provide uninterrupted energy, lower the cost of energy supply and investments, and offer cost-effective options. The focus is on determining the optimal sizing of the BESS to be used in the solar-based hybrid microgrid (SBH-MG).

This study utilizes real-world data on load profiles and solar generation to design and analyze an optimal SBH-MG. It is the first to employ both HOMER software and real reliability indices, offering a unique contribution by modeling existing solar home systems with a shared BESS using actual data. By incorporating power outage parameters from real-world conditions, this paper introduces a novel approach to researchers, modeling multiple solar homes shared through HOMER. The study explores the benefits of shared BESSs in reducing grid energy consumption, a topic that has received limited attention. It analyzes the technical and economic aspects of a microgrid's BESS, focusing on energy supply quality metrics such as SAIDI and system average interruption frequency index (SAIFI), contributing to a gap in the existing literature. Furthermore, the study presents an innovative multi-microgrid design with a shared BESS, examining energy costs and investment parameters. It explores potential system topologies in the electricity market under various pricing scenarios, providing researchers with a new perspective on this innovative approach.

II. METHODOLOGY

HOMER is utilized in this study as it fulfills the required tasks for three basic system design processes: simulation, optimization, and analysis.

A. HOMER Pro Software

HOMER software is a commercial computer program used to determine the specifications, planning, and sizing of system components, as well as their suitable capital costs, through technical and financial evaluation [26]. The flow chart in Fig. 3 illustrates how HOMER software determines the optimal dimensions and conducts an economic and technical analysis of renewable energy system equipment, utilizing the input data required for simulation.

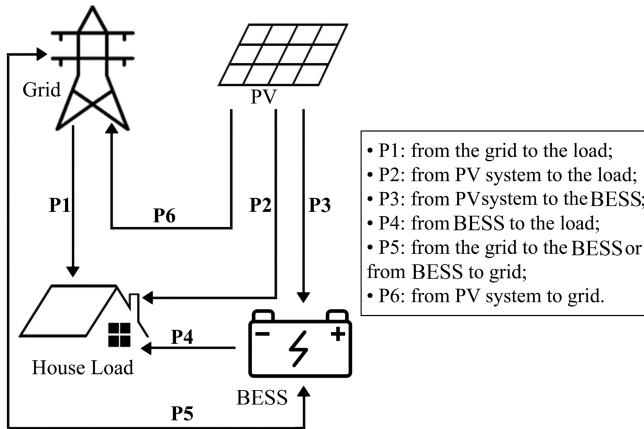


Fig. 1. Power flow schematic (adapted from [23]).

B. Pecan Street Data

Dataport is an online research database of residential energy data owned and operated by Pecan Street Inc., a nonprofit energy research institute headquartered at The University of Texas at Austin [28]. A view of the homes on Pecan Street is given in Fig. 4.

The electricity and consumption data of the solar home located on Pecan Street are used for the design and analysis to be carried out in this study. This study examines the annual power generation and consumption data from five solar homes located close to each other in Austin, Texas, in 2018.

The selected homes are in close proximity to each other, resulting in short electrical lines and low losses, allowing for the assumption of negligible line losses in this study [29-31].

The prosumer solar homes in Austin, Texas, are named A, B, C, D, and E. These homes are selected from the same geographical area,

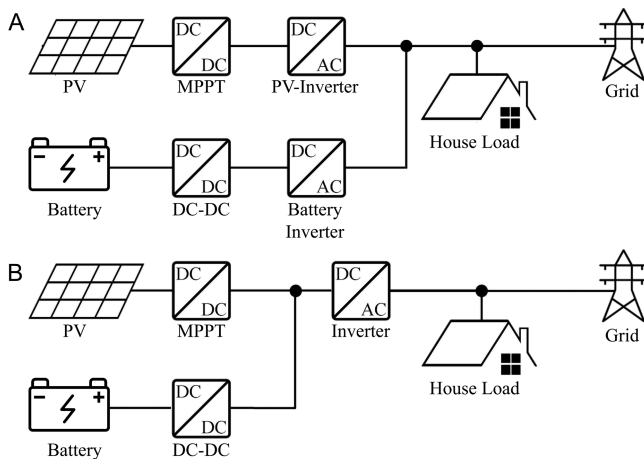


Fig. 2. Scheme of the connection topologies of the BESS a) AC-coupling of battery system, b) DC-coupling of battery system (adapted from [24]).

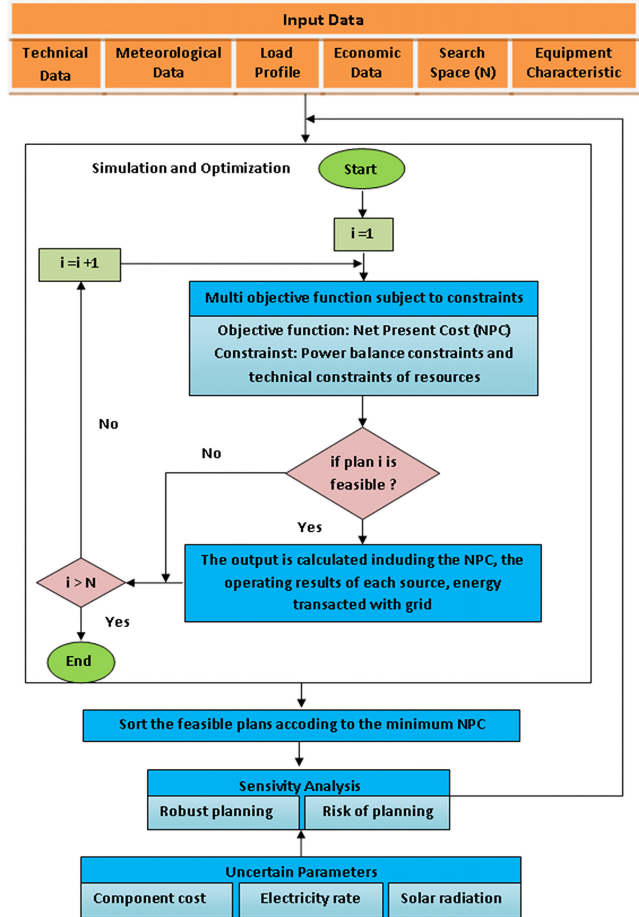


Fig. 3. The flowchart of HOMER optimization (adapted from [27]).

ensuring similar meteorological conditions. The characteristics of these homes make the feasibility of individual and shared BESSs possible. To achieve this, it is assumed that the houses are located in the same neighborhood.

The paper uses 15-minute interval data from 2018 for PV generation and demand load for five solar homes in the Austin region. Each simulation covered a 1-year period with 15-minute intervals. Load and PV generation profiles are shown in Fig. 5.



Fig. 4. The homes at Pecan Street are equipped with rooftop PV [28].

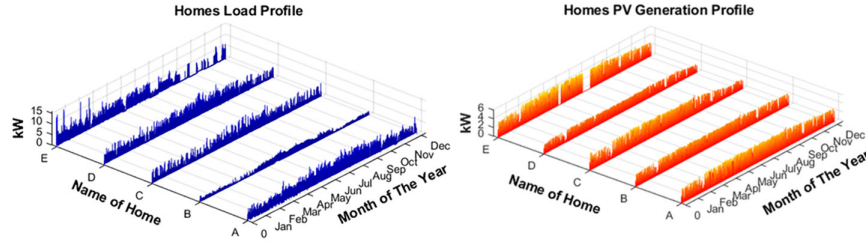


Fig. 5. Load and PV generation profiles for solar homes (01.01.2018–31.12.2018).

The HOMER system is designed to study the architecture with one BESS installed in each home, as shown in Fig. 6.

III. MATHEMATICAL FORMULATION

A. Equipment Characteristics

The characteristics of each piece of equipment, modeled in HOMER, determine the sizing and effective operation of the equipment in the SBH-MG. The characteristics of the SBH-MG equipment are described below.

1) Photovoltaic System

In this study, since real PV generation data is available, PV power is modeled as a generated power source in the optimization, using measured generation data from existing PV panels rather than calculating from irradiation.

2) Battery Energy Storage System

BESS stores surplus energy, providing power during outages and charging when PV generation exceeds demand, enhancing grid efficiency. The energy stored in the E_s is obtained by (1) [33].

$$E_r(t) = Ch_{bat}(t) \cdot \eta_{ch} \quad (1)$$

If the load requires more energy than the PV generation system can provide, the amount of energy released from the BESS at hour t is obtained using (2).

$$Dis_{bat}(t) = \frac{E_r(t)}{\eta_{dis}} \quad (2)$$

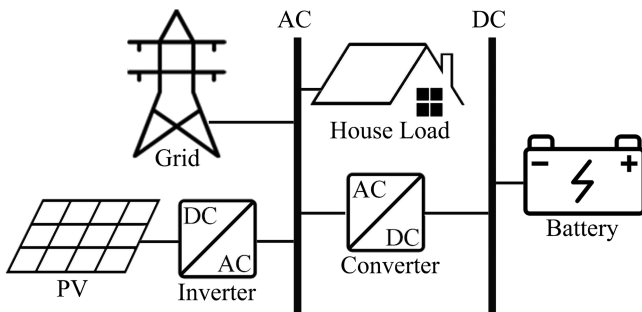


Fig. 6. HOMER Pro architecture for a sample house (adapted from [32])

where η_{ch} and η_{dis} are battery charge and discharge efficiency, respectively. The electrical energy accumulated in energy storage units is calculated by (3) [34].

$$E_{acc}(t) = E_{acc}(t-1) + Ch_{bat}(t) - Dis_{bat}(t) \quad (3)$$

where $E_{acc}(t)$ is accumulated electrical energy in the storage unit (Wh), $Ch_{bat}(t)$ and $Dis_{bat}(t)$ are battery charge and discharge energy, respectively. The number of batteries in the BESS is calculated by (4). The result is rounded up to the upper integer [35]

$$N_{bat} = \frac{E_{batt(max)} \cdot \Lambda_d}{I_{bat} \cdot V_{bat} \cdot DOD}, \quad (4)$$

where $E_{batt(max)}$ is the maximum electric energy accumulated in the storage system (Wh), Λ_d is the number of days, I_{bat} is the battery nominal capacity (Ah), V_{bat} is the battery bank voltage (V), and DOD is the depth of discharge (%) [33].

3) Power Converter

Converters are essential for converting PV-generated DC to AC (inversion) and vice versa (rectification) to supply AC loads. The power of converters is modeled as:

$$P_{inv,out} = \eta_{inv} \cdot P_{DC} \quad (5)$$

$$P_{rec,out} = \eta_{rec} \cdot P_{AC} \quad (6)$$

where $P_{inv,out}$ and $P_{rec,out}$ are the power output of the inverter and rectifier (kW), respectively. η_{inv} and η_{rec} are the inverter and rectifier efficiency (%), respectively. P_{AC} is the AC power input, and P_{DC} is the DC power input [36].

The specification of components used in the study are given in Table I, and their costs are given in Table II.

B. System Economics

The two principal economic elements, which are the total net present cost (NPC) and the levelized cost of energy (CoE), are related to the total annualized cost of the system [40]. HOMER aims to optimize the NPC and CoE.

1) Levelized Cost of Energy (CoE)

HOMER defines the CoE as the average cost per kWh of electrical energy for the SBH-MG. The CoE, which is the cost per kWh of the SBH-MG during a specified period of time, is obtained by (7) [41].

TABLE I.
 SPECIFICATIONS OF BESS AND CONVERTER

Battery	Specifications [37]
Brand/model	LGCHEM RESU
Nominal voltage	51.8 V
Nominal capacity	63 Ah
Roundtrip efficiency	>95%
Maximum charge current	71.4 A
Maximum discharge current	71.4 A
Nominal energy	3.3 kWh
Usable energy capacity	2.9 kWh
Lifetime	10 years
Minimum state of charge	12%
Converter	Specifications [38]
Inverter input efficiency	90%
Rectifier input efficiency	85%
Lifetime	15 years

$$CoE = \frac{C_A}{E_p + E_s} (\$/kWh) \quad (7)$$

where C_A is the total annual cost in (\$/yr), E_p is the amount of load that the system serves yearly (kWh/yr), and E_s is the amount of energy sold to the grid annually (kWh/yr). HOMER simulates all possible system configurations by changing the size of each system's equipment by means of a specified step within the defined search space. Among the system equipment sizings obtained from the simulation results, the optimal size of BESS is chosen based on its lowest CoE (\$/kWh).

2) Net Present Cost (NPC)

The total NPC of a power system is the difference between the present cost value spent during the life of the system equipment for the used energy and the present revenue of the energy which is generated by SBH-MG [42].

This spending value includes the energy costs purchased from the grid, the capital costs required for system installation, replacement

TABLE II.
 LIFETIME COST OF SYSTEM COMPONENTS

Component	Capital Cost	Replacement Cost	O&M Cost
BATTERY STORAGE	\$1 [37]	\$2500 [37]	\$7.3/yr [39]
SYSTEM CONVERTER	\$550/kW [38]	\$450/kW [38]	\$5/kW/yr [39]

O&M, operation and maintenance.

costs, and operation and maintenance (O&M) costs. On the other hand, the revenue includes salvage value and income from the sale of energy to the grid. The HOMER software separately calculates the NPC's total reduced cash flows for each year of the project life [43].

The total NPC is the main economic output of HOMER, which is based on the total annual cost and levelized energy cost ranking according to all system configurations. After entering load profiles and all component data, all possibilities of optimization results are obtained from HOMER, considering the NPC. The total annualized cost is calculated by (8).

$$C_A = C_c + C_r + C_{o\&m} + C_g - (R_s + R_g) \quad (8)$$

where C_A is the total annualized cost (\$/year), C_c is the capital cost, C_r is the replacement cost, $C_{o\&m}$ is the O&M cost, C_g is the cost of buying power from the grid, R_s is the salvage cost, and R_g is grid sales revenue. It is noted that the salvage cost is the remaining value of a component of the power system at the end of the project lifetime [44]. R_s is calculated by (9).

$$R_s = C_r \cdot \frac{R_{remaining}}{N_{lifespan}}, \quad (9)$$

where C_r is the replacement cost of the component, $R_{remaining}$ is the remaining life of the component, and $N_{lifespan}$ is the total life span of the component. The NPC is calculated by using (10) [36].

$$NPC = \frac{C_A}{CRF(i, N)}, \quad (10)$$

where i is the annual interest rate (%), N is the lifetime of the project (years), and CRF is the capital recovery factor. Capital recovery factor is calculated by (11) [41].

$$CRF(i, N) = \frac{i(1+i)^N}{(1+i)^N - 1} \quad (11)$$

C. Objective

The optimization approach specifies the objective functions and constraints to determine the optimal BESS capacity. By adopting this approach, the ideal values that minimize NPC and CoE for the created microgrid topologies will be determined for the simulation period [45]. The objective function that has to be minimized can be expressed as follows:

$$\text{ObjectiveFunction(OF)} = \min(\text{NetPresentCost}) \quad (12)$$

For analyzing the SBH-MG, NPC in solar homes and CoE are determined. The objective function is to determine NPC and CoE by means of the proposed system in HOMER.

D. Constraints

This study aims to determine the optimal microgrid topology design to provide users with optimal solutions within the given constraints.

1) Power Balance Constraint

The microgrid must satisfy the power balance in (13).

$$P_{load} = P_{pv} + P_{bat}^{dis} - P_{bat}^{char} + P_{grid}^{import} - P_{grid}^{export}, \quad (13)$$

where P_{load} is the total demand load, P_{pv} is the power of the PV system, $P_{bat}^{char} / P_{bat}^{dis}$ are the charging/discharging power of the BESS, and $P_{grid}^{import} / P_{grid}^{export}$ are the import/export power of the microgrid from or to the grid.

2) Battery Energy Storage System Constraint

The BESS capacity must be within the minimum and maximum capacity limits. The BESS constraints are mentioned as follows:

$$E_{batt,min} \leq E_{batt}(t) \leq E_{batt,max} \quad (14)$$

$$ON_{bat}, N_{bat} = \text{integer}, \quad (15)$$

where N_{bat} is the number of BESS.

3) Power Reliability Indices Constraints

Considering the power reliability in energy supply, the failure to meet the energy demand is expressed as the unmet load constraint in (16) [46].

$$\text{unmet load} = 1 - \frac{\text{yearly load supplied}}{\text{yearly demand load}} \quad (16)$$

The constraints and the economic parameters used in the proposed system are given in Table III.

IV. THE TOPOLOGY OF THE SOLAR HOMES

This study compared the total energy costs of shared and individual-use BESSs for grid-connected solar houses in the same region. Based on the results, the use of the BESS, whether individually or shared, will be evaluated in terms of economic and other factors. The schematic representation of solar homes' generation with individual and centrally shared BESSs is shown in Fig. 7.

V. ELECTRIC SYSTEM RELIABILITY INDICES

The quality of supply continuity, measured by outages and interruption duration, has become a critical indicator in some countries. Consequently, many countries use international standards like SAIDI and SAIFI, developed by the IEEE, to assess system performance [47].

TABLE III.

PROJECT CONSTRAINTS AND ECONOMIC PARAMETERS

Variable	Input For This Study
Nominal discount rate	8%
Project lifetime	25 years
Interest rate	2%
Annual capacity shortage	0%
Minimum renewable fraction	0%

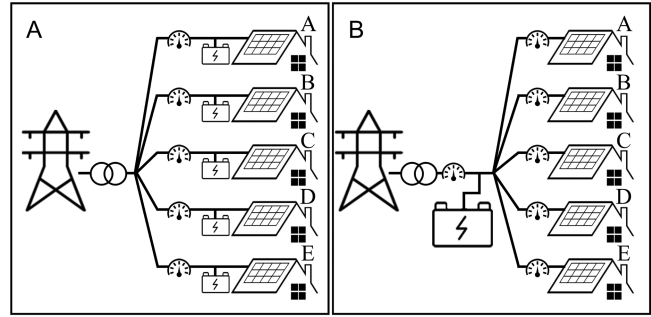


Fig. 7. Schematic representation of solar homes. (a) Individual BESS. (b) Central shared BESS.

System average interruption duration index is the system index of the mean period of interruption in the energy supply indicated in minutes per the demand of the customer in (17).

$$SAIDI = \frac{\sum \text{Customer Interruption Duration}}{\text{Total Number of Customers Served}} \quad (17)$$

System average interruption frequency index is a system index of the average frequency of interruptions in power supply in (18).

$$SAIFI = \frac{\sum \text{Total Number of Customers Interruptions}}{\text{Total Number of Customers Served}} \quad (18)$$

Customer average interruption duration index is a reliability index commonly used by electric power utilities. Customer average interruption duration index shows the mean of interrupted time that any given customer experiences. In other words, CAIDI gives the time required for the system to become energized again after the interruption in (19).

$$CAIDI = \frac{\sum \text{Customer Interruption Duration}}{\text{Total Number of Customers Interrupted}} \quad (19)$$

The reliability indices published by Austin Energy, the electricity power utility serving the region where the data are obtained, from 2018 to 2021 are presented in Table IV. The 2021 worst-case conditions data are used to demonstrate the impact of power outages on

TABLE IV.
RELIABILITY INDICES FOR PECAN STREET REGION OBTAINED FROM AUSTIN ENERGY [48]

Year	SAIFI (Times per year)	SAIDI (Minutes per year)	CAIDI (Minutes per interruption)
2021	1.89	1921.89	1016.87
2020	0.68	54.27	79.81
2019	1.00	86.42	86.42
2018	0.76	68.68	90.37

CAIDI, customer average interruption duration index; SAIDI, system average interruption duration index; SAIFI, system average interruption frequency index.

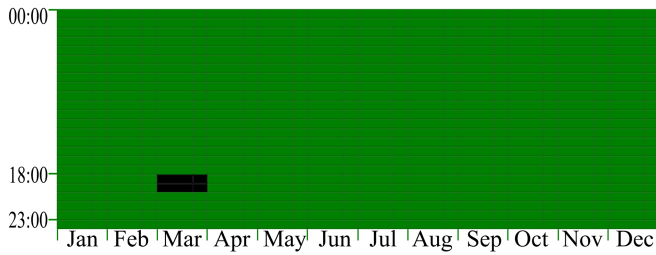


Fig. 8. The grid outages during the year.

the grid. In this study, SAIDI, SAIFI, and CAIDI were adapted to be simulated in HOMER for the grid outage schedule.

VI. THE ECONOMICAL EFFECTS OF BESS INTEGRATION AND OUTAGE

To demonstrate the effects of integrated BESS and grid outages on CoE and NPC, firstly, BESS is integrated into a selected solar home. Then, calculations are made assuming grid outages occur between 19:00 and 21:00 hours every day in March of a given year. In such cases, the BESS meets the load demand when the PV system does not generate sufficient power and the grid is unavailable.

Fig. 8 illustrates the hourly grid outages experienced by the distribution company, where black spots represent outages over the year and regular grid operation is shown in green.

For March 1–2, 2018, it was analyzed that PV, grid, and BESS collectively met the solar home’s load. The power variations for the scenarios of without-BESS, with-BESS, and with-BESS-grid outages are shown in Fig. 9 for these selected 2 days in the solar home.

In the first case (without BESS), the solar home meets its power needs solely from the grid and PV. From 00:00 to 06:00, the load is

supplied entirely by the grid. During the day, from 12:00 to 17:00, the excess electricity generated by the PV is sold to the grid, as the generation exceeds the demand load. Between 06:00 and 12:00, the solar home meets the demand load due to its lower cost and sells the excess generated power to the grid.

In the second case (with BESS), the system includes PV, BESS, and the grid. At 12:00, the excess power generated by the PV is used to charge the BESS instead of being sold to the grid. Once the BESS reaches its upper storage limit, the excess PV energy is then sold to the grid. During the high-price grid purchase period from 19:00 to 21:00 on March 1, 2018, the BESS discharges the previously stored energy to meet the load. The grid supplies any remaining power gap in case the BESS’s output is insufficient. On March 2, 2018, during similar hours, the load was fully met by the BESS, as the power required is lower.

In the third case (with BESS and grid outage), the system includes PV, BESS, and the grid to supply energy. The black spot indicates a grid outage throughout the hour. From 19:00 to 21:00 on the first and second days, a grid outage occurs and the PV does not generate any power, so the solar home does not buy power from the grid. As a result, the BESS starts to meet the load demand. The grid outage then disappeared at 21:00, and the demand load is supplied by both the BESS and the grid. To store energy, the BESS operates in charge mode from 22:00 to 23:00 on March 1–2, 2018.

The CoE is calculated as 0.036 \$/kWh without the BESS case, while the CoE is calculated as 0.032 \$/kWh in the case of the BESS integrated with the solar home system. As expected, integrating a BESS with the solar home reduces the CoE compared to a system without a BESS. However, when considering grid outages, the CoE is calculated to be 0.038 \$/kWh. The CoE inherently increases when compared to systems without BESS and with BESS, since more batteries and converter power are needed to supply energy uninterruptedly.

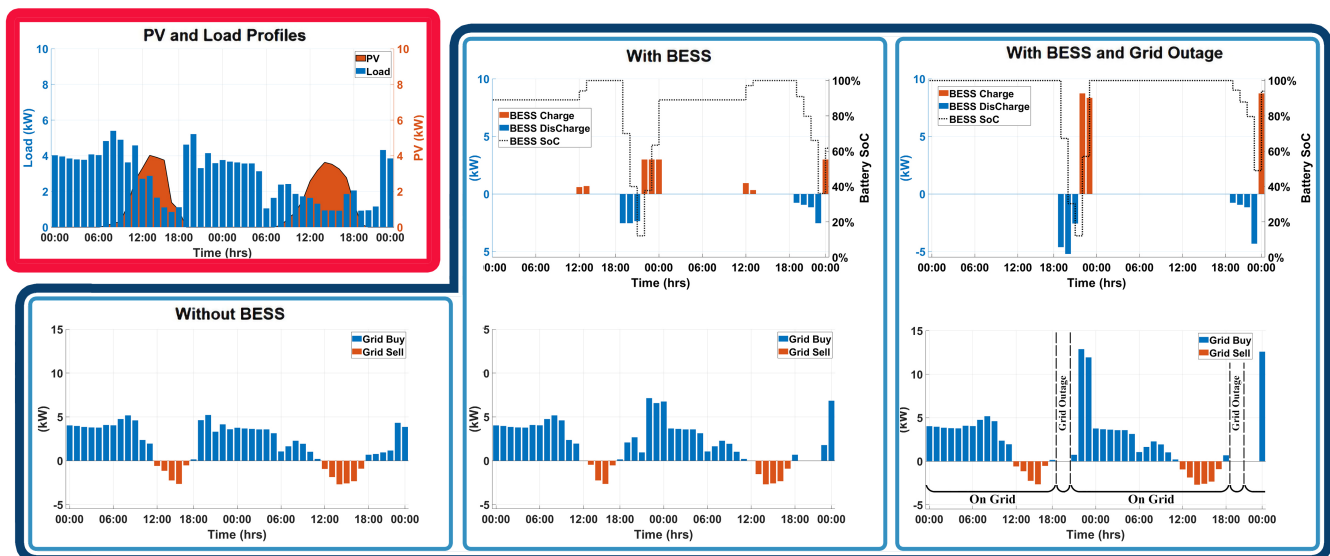


Fig. 9. The hourly power of without-BESS/with-BESS, with-BESS, and grid outage cases for selected 2 days (March 1–2, 2018).

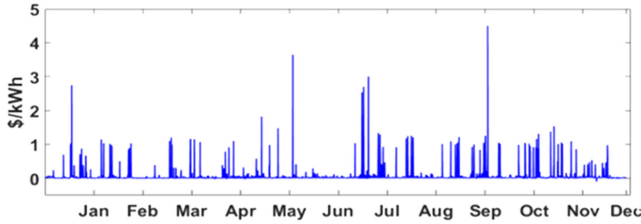


Fig. 10. Real-time prices for 2018, in Austin, TX, USA [30].

Similarly, the NPC is affected by the BESS and outage, with the NPC calculated as \$20 563, \$19 493, and \$21 718 for the systems with-out-BESS, with-BESS, and with-BESS-grid outage, respectively.

VII. THE CASE STUDIES

The paper investigates the BESS capacity requirements for solar home systems, comparing individual and shared BESS architecture models. Simulation studies are conducted using three different electricity pricing structures, resulting in a total of six case studies—three for individual batteries and three for shared batteries. For all case studies, the price of energy sold to the grid is assumed to be at a fixed rate.

Case-1: Real-time prices (RTP): Real-time pricing reflects current conditions and provides accurate information about the marginal power price in a region.

In Case-1, the individual BESS of five homes is compared to the central shared BESS, taking into account the real-time electricity price tariff. The fluctuations in real-time electricity prices are depicted in Fig. 10, which shows the price variations for 2018 at a 5-minute interval. Simulation studies are conducted using real load and PV power generation data for a number of residential prosumers, and comparisons are made between the shared and individual BESS.

Case-2: Flat price tariff (FPT): According to the flat price tariff, the energy purchase price is \$0.10/kWh for all hours while the energy sale price is \$0.04/kWh [28].

Case-3: Time of use tariff (ToU): Time-of-use pricing refers to electricity rates that vary throughout the day. Rates are typically divided into off-peak, mid-peak, and on-peak periods. The electricity costs for a solar home are calculated using the ToU rates shown in Table V [49].

TABLE V.

SCHEDULE’S TOU RATES AND HOURS FOR 2018, IN AUSTIN, TX, USA

ToU Period	Hours	Tariff (\$/kWh)
Off-peak	00:00–06:00	0.01188
	22:00–24:00	
Mid-peak	06:00–14:00	0.06218
	20:00–22:00	
On-peak	14:00–20:00	0.11003

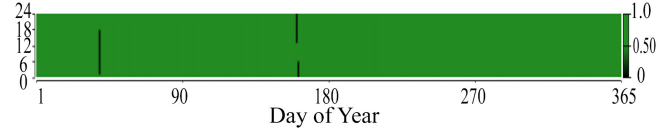


Fig. 11. The randomly generated grid outage chart.

Case-4: Considering reliability indices: This case study analyzes individual and shared BESS, considering different price tariffs and grid outages (SAIDI, SAIFI, and CAIDI). The Fig. 11 shows the power outages in the grid over 1 year, based on HOMER data, where green areas represent grid energy availability and black areas indicate outages.

The published data from electricity distribution companies, including SAIDI, SAIFI, and CAIDI, is used to determine the mean outage frequency and mean repair time required by the HOMER software. After inputting these reliability indices, HOMER generates a 1-year power outage graph, with the timing of outages pseudo-randomly chosen based on the provided indices.

VII. SIMULATION RESULTS

The proposed formulation for finding optimal BESS capacity that minimizes CoE and NPC, as presented in Section 3, is tested using two different topologies: the shared BESS and individual BESS configurations. The following figures show the optimization results obtained from HOMER. Fig. 12 depicts the case results of the SBH-MG, which have the centralized shared and the individual BESSs, considering cases 1, 2, and 3 with different price tariffs. The abbreviations from A to E shown in the graphs below represent the names given to the prosumer solar homes that are analyzed.

In case-1, which considered the real-time price tariff, the costs of energy for Customers A, B, C, D, and E are 0.032, 0.040, 0.038, 0.045, and 0.035 \$/kWh, respectively, in the individual topology. However, the CoE is \$0.020/kWh for the load profile created by the aggregation of loads in the shared topology. Fig. 12 depicts the CoE results for the other tariffs, case-2 and case-3.

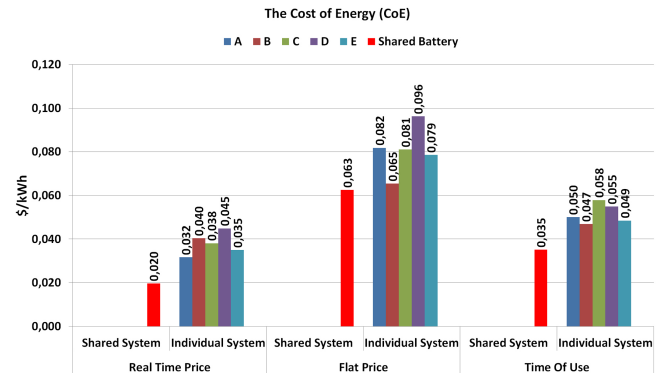


Fig. 12. Variation of cost of energy (CoE) for each house according to cases 1, 2, and 3.

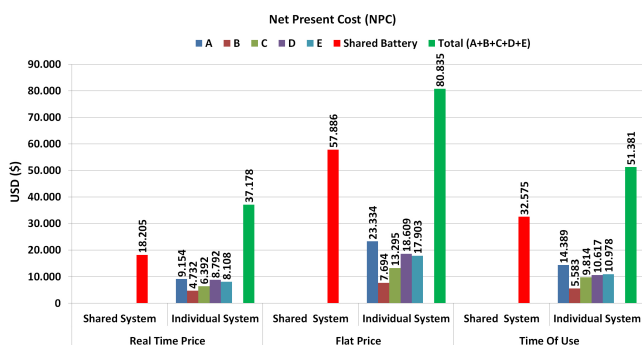


Fig. 13. Variation of net present cost (NPC) for each home according to cases 1, 2, and 3.

The shared BESS topology architecture had a lower CoE than the individual BESS topology across various market price tariffs. The CoE varies for each solar home due to their different load and PV profiles.

The simulation results for the NPC values are shown in Fig. 13. The NPC values calculated for solar homes A, B, C, D, and E are \$9154, \$4732, \$6339, \$8792, and \$8108, respectively, under the case-1 price tariff. While the total NPC value of all the solar homes in the individual topology is calculated as \$37 178, the NPC of the shared BESS is calculated as \$18 205. As the results show, the shared BESS topology has a lower NPC value compared to the individual BESS. The shared BESS's lower cost indicates it is more advantageous. The NPC values in case-2 and case-3 were also lower in the shared BESS topology, similar to case-1.

The results show that installing a shared BESS is more advantageous than individual BESS for the five solar homes in terms of NPC value.

Fig. 14 illustrates the amount of energy each home bought from and sold to the grid.

In case-1, the total energy purchased from the grid by all homes is calculated as 51 067 kWh in the individual BESS, whereas it is 43 655 kWh in the shared BESS. This indicates that the shared BESS system requires less energy from the grid than the individual BESS. Similarly, the analyses reveal that the solar homes with shared BESS topology

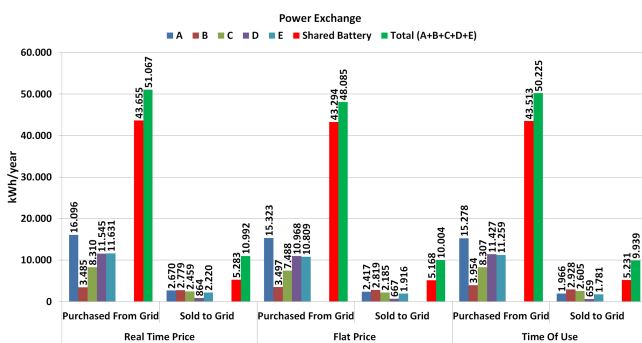


Fig. 14. Energy buying and selling of homes in cases 1, 2, and 3.

inject less energy into the grid than individual homes. The energy generated by solar homes is largely consumed within the system owing to the shared BESS connection topology, as suggested by these results.

This can help reduce the microgrid's dependency on the grid, which is a desirable operational method to mitigate the impact of grid outages. It is seen that a similar advantage is taken in all price tariffs.

Microgrid models often assume uninterrupted grid availability, but this is not the case in reality. Therefore, it is important to account for grid faults and interruptions during the design process, as they are common occurrences that can impact energy continuity. In case-4, similar to previous cases, two different subcases are designed. Firstly, the individual BESS topology is integrated into the solar homes, and then a shared BESS system is integrated into the demand aggregation point of five solar homes.

Considering the grid power outage given in case-4, different price tariffs are applied. According to the obtained simulation results, NPC, CoE, and the number of batteries are shown in Figs. 15-17, respectively.

In a RTP scenario, the sum of the individual NPC values of five homes is calculated as \$312 756, whereas the NPC value of aggregating five solar homes is calculated as \$283 182. According to the results obtained from cases 1–4, where RTP, flat-rate tariff, and ToU

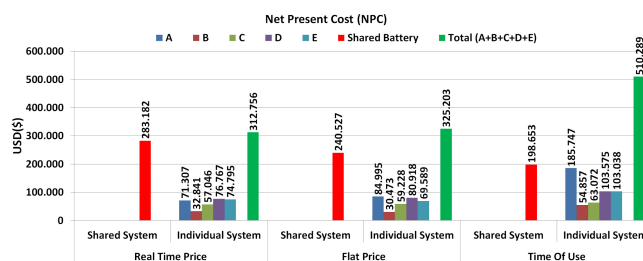


Fig. 15. In case-4, the change of NPC according to different price tariffs.

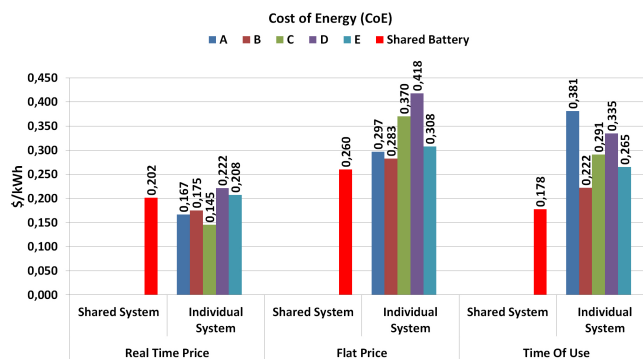


Fig. 16. In case-4, the change of CoE according to different price tariffs.

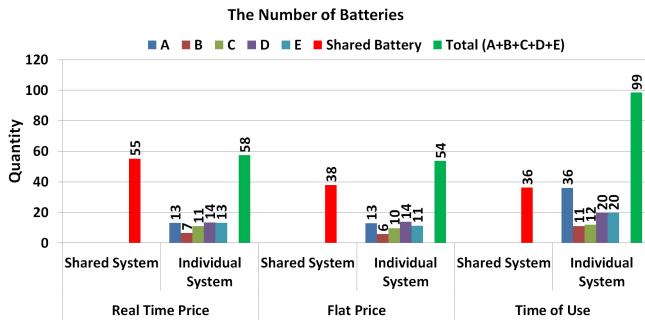


Fig. 17. In case-4, number of BESS according to different price tariffs for the average of ten trials.

are applied, the shared BESS topology is found to be significantly more advantageous in terms of the NPC compared to the individual BESS.

The CoE is mostly lower in the shared BESS topology compared to the individual BESS topology across different market price tariffs. Furthermore, the average of ten trials shows that the total number of individual batteries for five homes is 58, but the number of batteries in the aggregated system of five solar homes is 55, considering the grid outages in case-1. A similar advantage in the number of batteries is observed for the other cases, which are FPT and ToU in the shared BESS.

IX. CONCLUSION

The study demonstrates that shared BESS offers significant economic advantages over individual BESSs for prosumers. The shared BESS proved more cost-effective in terms of both CoE and NPC across various tariff structures (RTP, FPT, and ToU). Specifically, the shared BESS resulted in substantial cost reductions, with NPC values being 51%, 28%, and 37% lower than the individual system, under the RTP, FPT, and ToU tariffs, respectively.

Furthermore, the energy exchange between homes through the shared BESS leads to a decrease in the energy cost paid to the grid. For energy exchange, the amounts of energy imported from the grid are 15%, 10%, and 13% less in the shared BESS compared to the individual system under the RTP, FPT, and ToU tariffs, respectively, while the amount of energy injected into the grid are 52%, 48%, and 47% less in the shared BESS. This result indicates that in the shared BESS usage, the energy is provided for the use of neighboring homes instead of being sold to the grid.

The paper shows that the shared BESS is more advantageous compared to individual BESSs, particularly in ensuring continuous energy supply during grid outages. The NPCs for the shared BESS are 9%, 26%, and 61% lower compared to the individual BESS system under RTP, FPT, and ToU tariffs, respectively. Additionally, the shared BESS requires fewer batteries across all cases, indicating lower investment and operating costs. Overall, the shared BESS proves to be a more cost-effective and reliable solution, considering both price variations and grid reliability.

Availability of Data and Materials: The data that support the findings of this study are available on request from the corresponding author.

Peer-review: Externally peer-reviewed.

Author Contributions: Concept – S.P., E.B.; Design – S.P.; Supervision – E.B.; Resources – S.P., E.B.; Materials – S.P.; Data Collection and/or Processing – S.P.; Analysis and/or Interpretation – S.P., E.B.; Literature Search – S.P.; Writing – S.P., E.B.; Critical Review – S.P., E.B.

Declaration of Interests: The authors have no conflicts of interest to declare.

Funding: This study received no funding.

REFERENCES

- J. O. C. P. Pinto, and M. Moreto, "Protection strategy for fault detection in inverter-dominated low voltage AC microgrid," *Electr. Power Syst. Res.*, vol. 190, no. July, p. 106572, 2021. [\[CrossRef\]](#)
- R. Sabzehgar, M. A. Kazemi, M. Rasouli, and P. Fajri, "Cost optimization and reliability assessment of a microgrid with large-scale plug-in electric vehicles participating in demand response programs," *Int. J. Green Energy*, vol. 17, no. 2, pp. 127–136, 2020. [\[CrossRef\]](#)
- E. M. Esmail, N. I. Elkalashy, T. A. Kawady, A. M. I. Taalab, and M. A. Elsadd, "Modified autonomous fault management strategy for enhancing distribution network reliability," *Electr. Eng.*, vol. 89, no. 01234567, 2021.
- S. M. Shaahid, "Economic feasibility of decentralized hybrid photovoltaic-diesel technology in Saudi Arabia: A way forward for sustainable coastal development," *Therm. Sci.*, vol. 21, no. 1, pp. 745–756, 2017. [\[CrossRef\]](#)
- S. Talari, M. Shafie-khah, G. J. Osório, J. Aghaei, and J. P. S. Catalão, "Stochastic modelling of renewable energy sources from operators' point-of-view: A survey," *Renew. Sustain. Energy Rev.*, vol. 81, pp. 1953–1965, 2018. [\[CrossRef\]](#)
- M. Bartecka, P. Terlikowski, M. Klos, and Ł. Michalski, "Sizing of prosumer hybrid renewable energy systems in Poland," *Bull. Pol. Acad. Sci. Tech. Sci.*, vol. 68, no. 4, pp. 721–731, 2020. [\[CrossRef\]](#)
- M. Bagheri, N. Shirzadi, E. Bazdar, and C. A. Kennedy, "Optimal planning of hybrid renewable energy infrastructure for urban sustainability: Green Vancouver," *Renew. Sustain. Energy Rev.*, vol. 95, no. 2017, pp. 254–264, 2018. [\[CrossRef\]](#)
- G. Zhang, C. Xiao, and N. Razmjooy, "Optimal operational strategy of hybrid PV/wind renewable energy system using homer: A case study," *Int. J. Ambient Energy*, vol. 0, pp. 1–33, 2020.
- H. Z. Al Garni, and A. Garni, *Optimal Design and Analysis of Grid-Connected Solar Photovoltaic Systems* PhD thesis. Concordia University, 2018.
- S. Polat, and H. Sekerci, "The determination of optimal operating condition for an off-grid hybrid renewable energy based micro-grid: A case study in Izmir, Turkey," *Emitter Int. J. Eng. Technol.*, vol. 9, no. 1, pp. 137–153, 2021. [\[CrossRef\]](#)
- N. Yimen *et al.*, "Optimal design and sensitivity analysis of distributed biomass-based hybrid renewable energy systems for rural electrification: Case study of different photovoltaic/wind/battery-integrated options in Babadam, northern Cameroon," *IET Renew. Power Gener.*, vol. 16, no. 14, pp. 2939–2956, 2022. [\[CrossRef\]](#)
- F. Garcia-Torres, C. Bordons, J. Tobajas, R. Real-Calvo, I. Santiago, and S. Grieu, "Stochastic optimization of microgrids with hybrid energy storage systems for grid flexibility services considering energy forecast uncertainties," *IEEE Trans. Power Syst.*, vol. 36, no. 6, pp. 5537–5547, 2021. [\[CrossRef\]](#)

13. A. Mahmood, A. R. Butt, U. Mussadiq, R. Nawaz, R. Zafar, and S. Razzaq, "Energy sharing and management for prosumers in smart grid with integration of storage system," *ICSG*, vol. 2017, pp. 153–156, 2017. [\[CrossRef\]](#)
14. M. N. Akter, M. A. Mahmud, M. E. Haque, and A. M. T. Oo, "An optimal distributed energy management scheme for solving transactive energy sharing problems in residential microgrids," *Appl. Energy*, vol. 270, no. May, p. 115133, 2020. [\[CrossRef\]](#)
15. M. N. Akter, M. A. Mahmud, and A. M. T. Oo, "An optimal distributed transactive energy sharing approach for residential microgrids," in *IEEE Power Energy Soc. Gen. Meet.*, vol. 785, pp. 1–5, 2017. [\[CrossRef\]](#)
16. S. Nguyen, W. Peng, P. Sokolowski, D. Alahakoon, and X. Yu, "Optimizing rooftop photovoltaic distributed generation with battery storage for peer-to-peer energy trading," *Appl. Energy*, vol. 228, pp. 2567–2580, 2018. [\[CrossRef\]](#)
17. L. Yavuz, A. Önen, S. M. Mueyen, and I. Kamwa, "Transformation of microgrid to virtual power plant - A comprehensive review," *IET Gener. Transm. Distrib.*, vol. 13, no. 11, pp. 2077–2087, 2019.
18. H. J. Khasawneh, M. B. Mustafa, A. Al-Salaymeh, and M. Saidan, "Techno-economic evaluation of on-grid battery energy storage system in Jordan using homer pro," AEIT International Annual Conference, AEIT 2019, vol. 2019, 2019. [\[CrossRef\]](#)
19. J. Y. Kim *et al.*, "Cooperative control strategy of energy storage system and microsources for stabilizing the microgrid during islanded operation," *IEEE Trans. Power Electron.*, vol. 25, no. 12, pp. 3037–3048, 2010. [\[CrossRef\]](#)
20. B. Faessler, M. Schuler, M. Preißinger, and P. Kepplinger, "Battery storage systems as grid-balancing measure in low-voltage distribution grids with distributed generation," *Energies*, vol. 10, no. 12, 2017. [\[CrossRef\]](#)
21. K. H. Chua, Y. S. Lim, and S. Morris, "Energy storage system for peak shaving," *Int. J. Energy Sect. Manag.*, vol. 10, no. 1, pp. 3–18, 2016. [\[CrossRef\]](#)
22. T. A. Nguyen, and R. H. Byrne, "Maximizing the cost-savings for time-of-use and net-metering customers using behind-the-meter energy storage systems," North American Power Symposium, NAPS, 2017. [\[CrossRef\]](#)
23. P. A. Hohne, K. Kusakana, and B. P. Numbi, "Model validation and economic dispatch of a dual Axis pv tracking system connected to energy storage with grid connection: A case of a healthcare institution in South Africa," *J. Energy Storage*, vol. 32, p. 101986, 2020. [\[CrossRef\]](#)
24. C. N. Truong, M. Naumann, R. C. Karl, M. Müller, A. Jossen, and H. C. Hesse, "Economics of residential photovoltaic battery systems in Germany: The case of tesla's powerwall," *Batteries*, vol. 2, no. 2, 2016. [\[CrossRef\]](#)
25. M. Schimpe, N. Becker, T. Lahlou, H. C. Hesse, H. G. Herzog, and A. Jossen, "Energy efficiency evaluation of grid connection scenarios for stationary battery energy storage systems," *Energy Procedia*, vol. 155, pp. 77–101, 2018. [\[CrossRef\]](#)
26. Y. Sawle, S. C. Gupta, and A. K. Bohre, "Review of hybrid renewable energy systems with comparative analysis of off-grid hybrid system," *Renew. Sustain. Energy Rev.*, vol. 81, no. June, pp. 2217–2235, 2018. [\[CrossRef\]](#)
27. S. Ladide, A. E. L. Fathi, M. Bendaoud, H. Hihi, and K. Fatah, "Flexible design and assessment of a stand-alone hybrid renewable energy system: A case study Marrakech, Morocco," *Int. J. Renew. Energy Res.*, vol. 9, no. 4, pp. 2003–2022, 2019.
28. PecanStreet, "PecanStreet," 2023. [Online], *Pecan Street Inc Dataport Load Data*. Available: <https://www.pecanstreet.org/dataport>. [Accessed: 03-Mar-2023].
29. M. Afzalan, and F. Jazizadeh, "Quantification of demand-supply balancing capacity among prosumers and consumers: Community self-sufficiency assessment for energy trading," *Energies*, vol. 14, no. 14, 2021. [\[CrossRef\]](#)
30. J. Wang, L. Li, and J. Zhang, "Deep reinforcement learning for energy trading and load scheduling in residential peer-to-peer energy trading market," *Int. J. Electr. Power Energy Syst.*, vol. 147, no. December, 2023. [\[CrossRef\]](#)
31. Y. Wang *et al.*, "Autonomous energy community based on energy contract," *IET Gener. Transm. Distrib.*, vol. 14, no. 4, pp. 682–689, 2020. [\[CrossRef\]](#)
32. L. L. C. HOMER Energy, "HOMER Pro Version 3.7 User Manual," *Homer Energy. Colorado USA*, 2016, p. 416.
33. H. Zahboune, S. Zouggar, G. Krajacic, P. S. Varbanov, M. Elhafyani, and E. Ziani, "Optimal hybrid renewable energy design in autonomous system using Modified Electric System Cascade Analysis and Homer software," *Energy Convers. Manag.*, vol. 126, pp. 909–922, 2016. [\[CrossRef\]](#)
34. A. Haffaf, F. Lakdja, R. Meziane, and D. O. Abdeslam, "Study of economic and sustainable energy supply for water irrigation system (WIS)," *Sustain. Energy Grids Netw.*, vol. 25, p. 100412, 2021. [\[CrossRef\]](#)
35. E. A. Al-Ammar *et al.*, "Residential community load management based on optimal design of standalone HRES with model predictive control," *IEEE Access*, vol. 8, pp. 12542–12572, 2020. [\[CrossRef\]](#)
36. A. Baruah, M. Basu, and D. Amuley, "Modeling of an autonomous hybrid renewable energy system for electrification of a township: A case study for Sikkim, India," *Renew. Sustain. Energy Rev.*, vol. 135, 2021. [\[CrossRef\]](#)
37. "LG Chem RESU 3.3–48V lithium-ion storage battery." [Online]. Available: <https://www.europe-solarstore.com/lg-chem-resu-3-3-48v-lithium-ion-storage-battery.html>. [Accessed: 14-Apr-2023].
38. A. S. Aziz, M. F. N. Tajuddin, M. R. Adzman, M. A. M. Ramli, and S. Mekhilef, "Energy management and optimization of a PV/diesel/battery hybrid energy system using a combined dispatch strategy," *Sustainability*, vol. 11, no. 3, 2019. [\[CrossRef\]](#)
39. S. Mohseni, A. C. Brent, and D. Burmester, "Community resilience-oriented optimal micro-grid capacity expansion planning: The case of totarabank eco-village, New Zealand," *Energies*, vol. 13, no. 15, 2020. [\[CrossRef\]](#)
40. A. Haffaf, F. Lakdja, R. Meziane, and D. O. Abdeslam, "Study of economic and sustainable energy supply for water irrigation system (WIS)," *Sustain. Energy Grids Netw.*, vol. 25, p. 100412, 2021. [\[CrossRef\]](#)
41. S. Vendoti, M. Muralidhar, and R. Kiranmayi, "Techno-economic analysis of off-grid solar/wind/biogas/biomass/fuel cell/battery system for electrification in a cluster of villages by Homer software," *Environ. Dev. Sustain.*, vol. 89, 2020.
42. W. M. Amutha, and V. Rajini, "Techno-economic evaluation of various hybrid power systems for rural telecom," *Renew. Sustain. Energy Rev.*, vol. 43, pp. 553–561, 2015. [\[CrossRef\]](#)
43. A. M. Aly, A. M. Kassem, K. Sayed, and I. Abouhassan, "Design of micro-grid with flywheel energy storage system using Homer software for case study," *Proceedings of 2019 International Conference on Innovative Trends in Computer Engineering*, ITCE 2019, 2019, pp. 485–491. [\[CrossRef\]](#)
44. C. Nsengimana, X. T. Han, and L. L. Li, "Comparative analysis of reliable, feasible, and low-cost photovoltaic microgrid for a residential load in Rwanda," *Int. J. Photoenergy*, vol. 2020, 1–14, 2020. [\[CrossRef\]](#)
45. M. Ali *et al.*, "Techno-economic assessment and sustainability impact of hybrid energy systems in Gilgit-Baltistan, Pakistan," *Energy Rep.*, vol. 7, pp. 2546–2562, 2021. [\[CrossRef\]](#)
46. V. Suresh, M. Muralidhar, and R. Kiranmayi, "Modelling and optimization of an off-grid hybrid renewable energy system for electrification in a rural areas," *Energy Rep.*, vol. 6, pp. 594–604, 2020. [\[CrossRef\]](#)
47. D., "Subcommittee," *IEEE Guide for Electric Power Distribution Reliability Indices Distribution*, vol. 1997, pp. 1–4, 2012.
48. U.S. Electricity Information Administration, *EIA 861 - Annual Electric Power Industry Report*. Washington, DC, USA: US Energy Information Administration, 2015.
49. Austin City Council, *City of Austin Fiscal Year 2018 Electric Tariff*, 2018, pp. 1–49.